STABILIZING THE DEPTH OF A TOWED UNDERWATER VEHICLE UNDER THE IMPACT OF RANDOM SEA WAVES

Dang Nguyen Phu[1]*, Tuan Vu Duc[2]

[1]*Military Technical Academy, Vietnam*
[2]*University of Transport Technology, Vietnam*

*Corresponding author: npdang@lqdtu.edu.vn

(Received: February 19, 2024; Revised: September 17, 2024; Accepted: September 27, 2024)

DOI: 10.31130/ud-jst.2024.054E

Abstract - Stabilizing the depth of the Towed Underwater Vehicle (TUV) under the impact of ocean waves is the first problem when building a control and monitoring system for TUV. Many strategies and control methods have been proposed in different studies, but they are not a general standard. Therefore, this research will propose and investigate a solution for synthesizing the control system to stabilize the TUV based on the real interpolation method (RIM) with the main contents: modeling the Towed cable (TC) - Underwater vehicle (UV) system, proposing the structure of the control system and the synthesis procedure of the regulators based on the RIM, building a synthesis program with different TC lengths. The simulation results show that the TUV exhibits good performance under the impact of sea wave. They can be applied to build the experimental models of TUV.

Key words - Towed Underwater Vehicle (TUV); Real Interpolation Method (RIM); Transfer Function (TF); Object with distributed parameters; Sea wave; Control system.

1. Introduction

Nowadays, TUVs, such as exploration equipment, seabed monitoring equipment, etc., are widely used in ocean research because of their outstanding advantages. The Ship - Cable - Underwater Vehicle system, in terms of stabilizing the position of UV, is a complex system strongly influenced by the marine environment, such as ocean currents, wind, and especially ocean waves.

In the Towing Cable - Underwater Vehicle (TC - UV) system, the TC is an element with distributed parameters whose processes are described by complex equations such as partial differential equations, integral equations, differential-integral equations, and other forms. Therefore, the transfer function relating to the displacement of the cable end attached to the UV and the displacement at the cable end attached to the winch contains not only high-order rational fractions but also delay and transcendental components, which have strong nonlinearity [1]:

$$W_{dt}(s) = f(s, e^{\frac{A(s)}{B(s)}}, \sqrt{s}, \cos(s), \sin(s), sh(s), ch(s), ...) \qquad (1)$$

Controlling the such objects (1) is a complex scientific problem.

The modeling and control of the TUV has been investigated in many studies. Research [2, 3] uses the lumped mass approximation method, while [4-6] uses classical cable theory based on the finite element method for modeling the towed cable. However, this method requires dividing the cable into many segments to obtain accurate simulation results and uses non-linear numerical models built by decomposing the vehicle into its constituent elements. The works [7-9] use the Absolute Nodal Coordinate Formulation (ANCF) method for modeling the cable dynamics. This method uses a constant mass matrix in the equation formulation, giving more accurate results with fewer cable segments than the finite element method.

Modeling and estimation of random sea waves using Gaussian white noise and shaping filter are presented in the researches [10-13], and the works [14-17] investigated the lurch of the ship and the influence of sea waves on the working depth of the TUV.

Research [18] proposes a nonlinear Lyapunov-based, adaptive output feedback control law, which stabilizes the pitch, yaw, and depth of the TUV using a nonlinear observer for estimating the linear velocities. [19-21] proposed a new hydrodynamic model to study the dynamic characteristics of TUV in different operating modes and a PID control model for depth tracking. The researches [22, 23] implemented a controller for compensating the influence of sea waves in the vertical plane for the autonomous underwater vehicle based on a modified linear quadratic Gaussian combined with a wave filter. In addition, there are other control methods for stabilizing the TUV, such as adaptive control, sliding control, feedback control based on observers, and other approaches and studies.

The above methods have solved the problem in many different aspects with positive results. However, they have complicated calculation procedures and large errors and are not a common technical standard. Therefore, this study will propose and investigate a solution to synthesize and calibrate the regulator using the real interpolation method [24, 25]. This method has a simple procedure, allowing direct manipulation of the original model (1) in the real domain and thus reducing the amount of calculation while preserving the specific features and effects of the objects with distributed parameters. This research will resolve the following main issues: Establishing the structure diagram of the TUV control system; Building the algorithm and synthesis program of controllers based on real interpolation method to stabilize the depth of TUV under the impact of random sea ocean waves; Simulating and evaluating the synthesized system with different cable lengths and wave levels.

2. Problem

2.1. Modeling the Towed Underwater Vehicle (TUV)

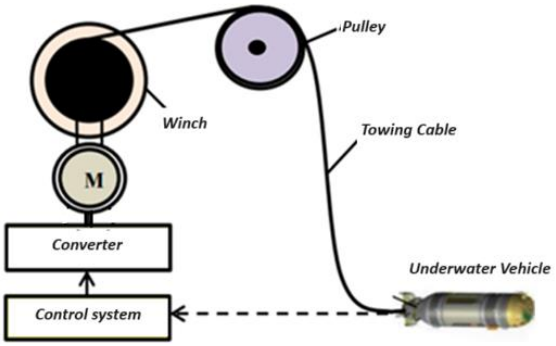

Figure 1. *General structure of the TUV control system*

The general structure of the TUV control system (Figure 1) includes the main components: the control system, the inverter-motor, the winch - pulley, and the system of towed cable - underwater vehicle. In which, the TC is an element with distributed parameters, whose processes are described by complex equations such as partial differential equations, integral equations, differential - integral equations and other forms.

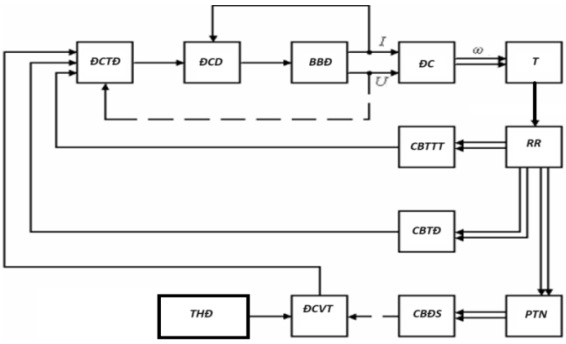

Figure 2*. Functional diagram of the TUV combined control system (DC- Motor; RR- Pulley; CBTTT- Speed sensor of ship lurch; CBĐS- Depth sensor of the UV; PTN- The system TC - UV; DCD- Current regulator; DCTĐ- Speed regulator; DCVT- position regulator; T- Winch; CBTĐ- Pulley speed sensor; BBD- Thyristor converter; THD - Input signal)*

A combined control system is often used to stabilize the UV position. It allows adjustment of both the noise and the displacement of the UV. This system has a functional diagram, as shown in Figure 2. The displacement signal of the UV is measured by the depth sensor (CBĐS) mounted on the UV and will be transmitted to the control system via cable.

2.1.1. Modeling the TC-UV system

To model the TC - UV system in the form of TFs, which associate between displacement at the end of the cable attached to the UV $x(L,s)$ and traction at the cable's point attached to the winches $T(0,s)$ with displacement at the cable's point attached to the winches $x(0,s)$, we'll consider a piece of cable as its axis coincides with the axis Oz when impacting the traction T, z is the cable's length without load, y and $x = y - z$ are cable's length and its deformation with load (Figure 3) respectively. The TC-UV system is affected by main forces: Weight of the TC-UV system in the water, elastic force, inertial force, frictional force between the cable with water and the cable's frictional force.

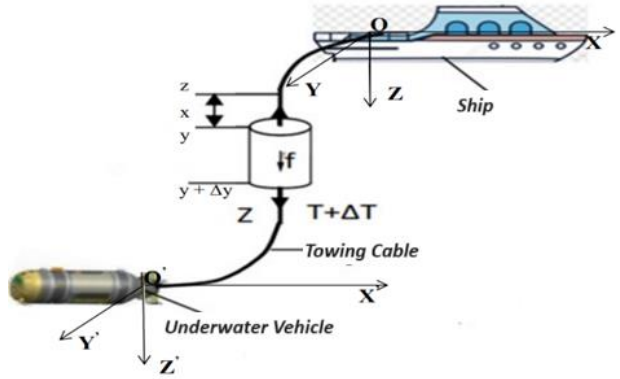

Figure 3. *The surveyed model of the cable´s piece and its deformation*

The vertical oscillation of the cable is described by a system of equations [15-17]:

$$\begin{cases} T = E_T.F.\partial x/\partial z + \lambda.F.\partial^2 x/\partial z.\partial t \\ \partial T/\partial z = m.\partial^2 x/\partial t^2 + \beta.\partial x/\partial t \end{cases} \quad (2)$$

where, E_T - Elastic modulus of the cable, F - the cable cross-section; λ - friction coefficient of the cable; m - mass of a cable's length per measurement unit (kg); β - the friction coefficient between the cable with water (s^{-1}).

After performing the Laplace transform with substitution $\lambda = E_T.\tau_{mp}$, the system of equations (2) becomes:

$$\begin{cases} \partial T/\partial z = m.s^2.x(z,s) + \beta.s.x(z,s) \\ T = E_T.F.(1+\tau_{mp}.s).\partial x(z,s)/\partial z \end{cases} \quad (3)$$

Based on the calculation results in [15-17], we get the TF, which associates between the displacement at the end of cable attached to the UV ($x(L,s)$) with displacement at the end of cable attached to the winches ($x(0,s)$):

$$W_{dt}(s) = \frac{x(L,s)}{x(0,s)} = \left(ch(\tau_L.r(s)) + \frac{m_{no}.s^2 + k_{no}.s}{Z_w(s)}.sh(\tau_L.r(s)) \right)^{-1} \quad (4)$$

with, $\tau_L = L/w$ - the wave propagation time in the cable; $Z_w(s) = b_w\sqrt{(s^2 + \nu_{mp}.s)(1+\tau_{mp}.s)}$, $b_w = m_d.w$ - the wave impedance (m_d - the mass per unit length of cable, $w = \sqrt{E_T.F/m}$ - the wave propagation speed in the cable (m/s); τ_{mp} - the time constant of internal friction (s); $r(s) = \sqrt{(s^2 + \nu_{mp}.s)/(1+\tau_{mp}.s)}$ - the fluctuation propagation coefficient; $\nu_{mp} = \beta/m$ - the relative drag coefficient along the cable (1/s); k_{no} - the coefficient of water resistance due to vehicle movement; m_{no} - the mass of UV in the water. When using a "KGP-1-20" cable and a UV with parameters: external diameter: Φ = 23.4mm; $m = 1.63kg/m$; $w = 4020m/s$; $\tau_{mp} = 0.01s$; $\beta = 0.05s^{-1}$;

$k_{no} = 1800kg/s; m_{no} = 5860kg$, the TF (4) will have the form:

$$W_{dt}(s) = \left(ch\left(\frac{L}{4020}\sqrt{\frac{s^2+0.0307s}{1+0.01s}}\right) + \frac{5860.s^2+1800.s}{6552.6.\sqrt{(s^2+0.0307s)(1+0.01s)}}.sh\left(\frac{L}{4020}\sqrt{\frac{s^2+0.0307s}{1+0.01s}}\right)\right)^{-1} \quad (5)$$

2.1.2. Modeling the impact of sea waves on TUV

The TUVs are affected by many different forces and moments such as ocean waves, ocean currents, wind and many other uncertain factors during operation. Sea waves are a factor that greatly affects the stability of TUVs. Under the influence of sea waves, the end of cable attached to the winch will fluctuate. The vertical oscillation components (according to the OZ axis) will affect the UV, while the horizontal oscillation components (according to the OX,OY axis) are ignored because of their rapid decrease under the influence of water resistance.

The block that transforms the white noise $N\ t$ into a random ocean wave $\zeta(t)$ is described by the TF [16]:

$$W_f(s) = \frac{3.694s^3}{(s^2+0.5111s+0.7208)(s^2+0.9465s+1.136)(s^2+1.974s+3.425)} \quad (6)$$

The ship's lurch ($X_K(s)$) caused by ocean waves is represented by a transfer function relating the vertical displacement at the end of cable attached to the winches ($x(0,s)$) and the wave peak $\zeta(s)$ [16]:

$$W_\zeta(s) = \frac{X_K(s)}{\zeta(s)} = \frac{x(0,s)}{\zeta(s)} = \frac{1}{s^2+0.866s+1} \quad (7)$$

The influence of ocean waves on the UV is represented by the transfer function:

$$W(s) = W_f(s)W_\zeta(s)W_{dt}(s) \quad (8)$$

2.1.3. Modeling the winch - pulley

The structure of the winch - pulley system is shown in Figure 4. When ignoring elastic and inertial properties, the force on the cable between the winder and the pulley is considered unchanged at every point of the cable. The displacement velocity of the point attached to the winches is determined by the expression:

$$V(0) = V_R + V_L = V_R + R_L \cdot \omega_L \quad (9)$$

where R_L and ω_L - the radius and angular velocity of the winch. When the winch is stationary ($V_L = 0$), the pulley's velocity (V_R) is the impact of ocean waves on the Winch - Cable - Vehicle system. The winch - pulley system is described by the TF [17]:

$$W_W(s) = \frac{2\pi R_L}{i.s} \quad (10)$$

The inverter – motor are described by the TFs:

$$W_{In}(s) = \frac{K_{In}}{T_{In}s+1}; W_M(s) = \frac{1/R_a}{T_a s+1}.\frac{C_M}{Js}, C_M = \frac{M_r}{I_a} = \frac{30P_r}{\pi N_r I_a} \quad (11)$$

with: K_{In}, T_{In} - gain and time constant of the inverter; $T_a = L_a / R_a$ - electromagnetic time constant of the motor (R_a - armature resistance of the motor, - L_a armature inductance of the motor); J - inertia moment of the motor; C_M - mechanical constant of the motor; P_r, N_r - rated power and rated speed of the motor; I_a - Rated armature current of the motor.

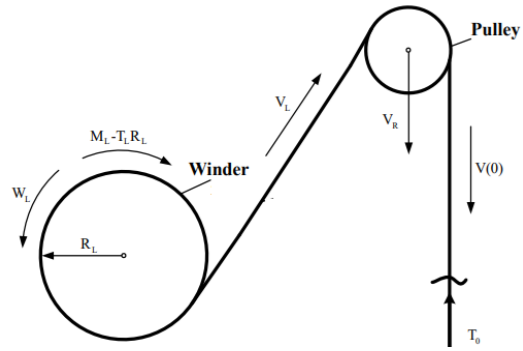

Figure 4. *Structural model of the winch - pulley system*

Based on the descriptions of the TC – UV (5), the winch – pulley (10) and the inverter – motor systems (11), the structural diagram of the control system stabilizing the depth of UV under the impact of ocean waves is shown in Figure 5, where $W_C(s), W_S(s), W_P(s)$ - regulators of the current, speed and position loops respectively; $W_{dt}(s)$ - the TF describing the TC – UV system; K_C, K_S, K_P - feedback coefficients; $X_K(s)$ - the ship's lurch is caused by ocean waves (6); $X(0,s), X(L,s)$ - The displacements of the end of cable attached to the winche and the UV respectively; $h_g(t)$ - input signal of system). The noise $X_K(s)$ introduced into the control system through a block with a TF $W_N\ s$ [17]:

$$W_N(s) = \frac{K}{s} \quad (12)$$

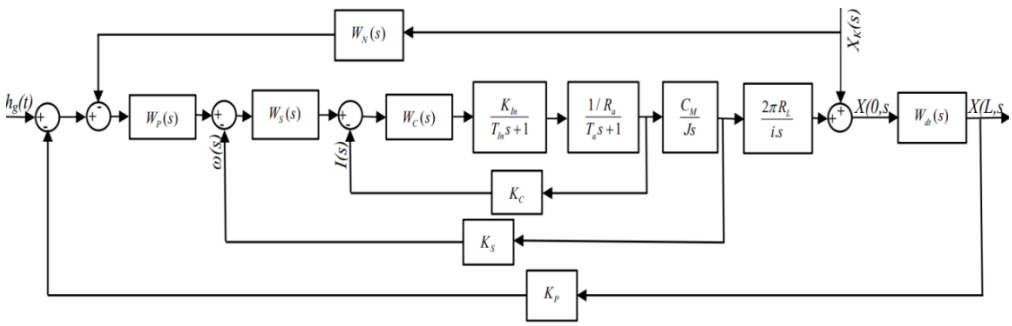

Figure 5. *The control system stabilizing the depth of TUV under the impact of ocean waves*

2.2. Synthesis of the controllers

2.2.1. Set up the synthesis algorithm

The task is to determine the regulators $W_{đc}(s)$:

$$W_{đc}(s)=\frac{b_m s^m+b_{m-1}s^{m-1}+...+b_1 s+b_0}{a_n s^n+a_{n-1}s^{n-1}+...+a_1 s+1} \quad (13)$$

and the feedback coefficient (K_{ht}) so that each loop satisfy the condition:

$$\begin{cases}\sigma_{yc}-\Delta\sigma\le\sigma_{th}\le\sigma_{yc}+\Delta\sigma\\ t_{qd}^{th}\le t_{qd}^{yc}\end{cases} \quad (14)$$

or

$$\begin{cases}\sigma_{yc}-\Delta\sigma\le\sigma_{th}\le\sigma_{yc}+\Delta\sigma\\ t_{qd}^{th}\to t_{qd}^{\min}\end{cases} \quad (15)$$

with, σ_{yc} - the overshoot of the desired system; σ_{th} - the overshoot of the synthesized system; $\Delta\sigma$ - the allowable overshoot erroneous; t_{qd}^{yc} - the settling time of the desired system; $t_{qd}^{th}, t_{qd}^{\min}$ - the settling time and the minimum achievable settling time of the synthesized system, respectively. In fact, when there is no regulator (13) for the system to satisfy the condition (14), we can move to condition (15), where the overshoot complies with the tight limit and also the excessive time is minimal (which is still larger than the required value). The transition from condition (14) to (15) ensures that the synthesis problem always has a solution without losing its generality.

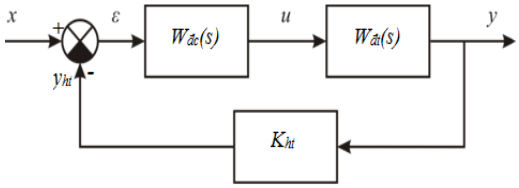

Figure 6. *Structure diagram of a single-loop automatic control system*

The synthesis equations corresponding to the single-loop control system (Figure 6) will have the form:

$$\begin{aligned}&W_{mm}^k(s)\cong W_{th}^k(s);W_{th}^k(s)=\frac{W_{đc}(s)W_{đt}(s)}{1+W_{đc}(s)W_{đt}(s)K_{ht}}\\ &W_{mm}^h(s)\cong W_{th}^h(s)=W_{đc}(s)W_{đt}(s);W_{mm}^h(s)=\frac{W_{mm}^k(s)}{1-W_{mm}^k(s)K_{ht}}\end{aligned} \quad (16)$$

where, $W_{mm}^k(s);W_{mm}^h(s)$ - the desired TF of the closed system and the open system respectively; $W_{th}^k(s);W_{th}^h(s)$ - The synthesized TFs of closed and open systems respectively.

To establish the synthesis algorithm based on the real interpolation method (RIM) [24,25], the synthesis equations (16) are first converted to equivalent form:

$$\begin{aligned}&W_{đc}(s)\cong\frac{W_{mm}^k(s)}{W_{đt}(s)-W_{đt}(s)W_{mm}^k(s)K_{ht}}.\\ &W_{đc}(s)\cong W_{mm}^h(s)/W_{đt}(s)\end{aligned} \quad (17)$$

The steps to solve the synthesis equations (14) based on RIM include: Determining the feedback coefficient K_{ht}; Finding the desired transfer function of system according to the required criteria σ_{yc}, t_{qd}^{yc}; Seting up and solving the equation (17) in the real domain; Calibrating the synthesized system.

a. Determining the feedback coefficient K_{ht}:

The feedback coefficient K_{ht} can be determined from the static mode of the system:

$$K<\frac{1}{H^{\infty}-\Delta H} \quad (18)$$

with, ΔH - the error in the established mode.

b. Determining the desired transfer functions:

One of the direct methods that allows determining the desired TF $W_{mm}^k(s)$ based on the required quality criteria σ_{yc} and t_{qd}^{yc} will be of the form [25]:

$$W_{mm}^k(s)=\frac{\frac{\alpha_1}{2}s+1}{\alpha_0 s^2+\alpha_1 s+1}H_{\infty};\alpha_0=\frac{[\ln(\frac{H_{\max}}{H_{\infty}}-1)]^2}{\frac{9}{t_{qd}^{yc^2}}\{[\ln(\frac{H_{\max}}{H_{\infty}}-1)]+\pi^2\}};\alpha_1=\frac{6\alpha_0}{t_{qd}^{yc}}, \quad (19)$$

with: H_{∞} - settling output signal in steady state; $H_{\max}$ – the maximum impulse response is determined from the relation: $\sigma_{yc}=\frac{H_{\max}-H_{\infty}}{H_{\infty}}100\%$.

c. Seting up and solving the synthesis equation:

To solve equation (17) based on RIM, it is first necessary to convert it to the form in terms of real variables δ:

$$W_{đc}(\delta)\cong\frac{W_{mm}^k(\delta)}{W_{đt}(\delta)-W_{đt}(\delta)W_{mm}^k(\delta)K_{ht}}. \quad (20)$$

After that, it is necessary to find the numerical characteristics of the functions in (20) with interpolation nodes $\delta_i(i=\overline{1,\eta};\eta=m+n+1)$ according to a certain rule.

In this research, the interpolation nodes $\{\delta_i\}_{\eta}$ are established to coincide with the zero points of the Chebyshev polynomials to increase the total accuracy [26]:

$$\delta_i=\frac{1+x_i}{1-x_i}a, i=\overline{1,\eta} \quad (21)$$

with: a – The real parameter; $\{x_i\}_{\eta}$ - the roots of the equation [26]:

$$\begin{aligned}&T_{\eta}(x)=0\\ &T_0(x)=1;T_1(x)=x;T_2(x)=x^2-\frac{1}{2};...;T_{\eta+1}(x)=xT_{\eta}(x)-\frac{1}{4}T_{\eta-1}(x);x\in[-1,1]\end{aligned} \quad (22)$$

Finally, the coefficients (a_i, b_j) of the regulator (13) are determined by solving the system of equations:

$$\begin{aligned}W_{đc}(\delta_i)&=\frac{b_m\delta_i^m+b_{m-1}\delta_i^{m-1}+...+b_1\delta_i+b_0}{a_n\delta_i^n+a_{n-1}\delta_i^{n-1}+...+a_1\delta_i+1}\\ &=\frac{W_{mm}^k(\delta_i)}{W_{đt}(\delta_i)-W_{đt}(\delta_i)W_{mm}^k(\delta_i)K_{ht}};i=\overline{1,\eta}\end{aligned} \quad (23)$$

d. Calibrating the synthesized system.

The main ways to calibrate the received system include:

- *Changing the interpolation nodes*

The essence of this method is to repeat the calculation steps with new interpolation nodes until the synthesized system has quality criteria that satisfy the requirements (14) or (15) ($\delta_i^{(k+1)} = \delta_i^{(k)} + \Delta\delta, i = 1 \div \eta$; $\delta_i^{(k)}$ - the interpolation nodes at the kth iteration; $\delta_i^{(k+1)}$ - the interpolation nodes at the k+1th iteration).

- *Changing the desired settling time (t_{qd}^{yc})*

In fact, increasing/decreasing the overshoot or the settling time will change the remaining criteria. Therefore, we will use the settling time as an instrumental variable to correct the overshoot. In this way, it is necessary to determine the relationship of the overshoot σ_{th} and the settling time t_{qd}^{yc} ($\sigma_{th} = f(t_{qd}^{yc})$). Then, we need to adjust the settling time t_{qd}^{yc} until the received overshoot σ_{th} satisfies the condition (14) or (15). Frequently, the overshoot σ_{th} will gradually decrease as the desired settling time t_{qd}^{yc} increases.

- *Changing the desired overshoot (σ_{yc})*

When the overshoot of the synthesized system (σ_{th}) is smaller or larger than the desired value (σ_{yc}), we can correct it by changing the desired overshoot (σ_{yc}) in the neighborhood of the given overshoot. Reality shows that, when $\sigma_{th} > \sigma_{yc} + \Delta\sigma_{yc}$, it is necessary to reduce the desired overshoot ($\sigma_{yc} \to \sigma_{yc\_\min}$). Otherwise, the desired overshoot should be increased ($\sigma_{yc} \to \sigma_{yc\_\max}$).

- *Using the special weight functions ($w(t)$)*

Another way of calibration is to use special functions (for example: $w(t) = e^{-\delta t}(1 - e^{-\delta t})$) to change the dynamic properties of the synthesized system when changing the interpolation nodes ($\delta_i, i = 1,2...$). This allows to achieve the required overshoot without having to change the desired criteria σ_{yc}, t_{qd}^{yc}.

From the above analysis, the synthesis procedure using RIM includes the following steps:

Step 1. Choosing the regulators $W_C(s), W_S(s), W_P(s)$ according to (13).

Step 2. Establishing the interpolation nodes $\delta_i, i = \overline{1,\eta}$ from condition (21).

Step 3. Calculating the numerical characteristics, setting up and solving the system of equations (23).

Step 4. Determining the overshoot and settling time of the synthesized system. Checking the condition (14) or (15).

Step 5. Repeat step 2 with different interpolation nodes $\delta_i, i = \overline{1,\eta}$ or step 1 with different structural parameters m, n until obtaining a regulator that creates a corresponding system satisfying the condition (14) or (15).

2.2.2. Synthesis of the control system stabilizing the depth of TUV under the impact of ocean waves

In this study, it is assumed that the system consists of separate control loops that do not influence each other. Each loop is synthesized separately from the inner loop to the outer loop [2]. With the structure diagram in Figure 5, the control system includes three control loops: current, speed and position.

Table 1. *The parameters of the TC – UV system and motor – inverter*

Motor D-816		**Towed Cable – Underwater Vehicle**	
Parameters	Value	Mass of a unit length of cable	$m = 1,63(kg/\mathrm{m})$
Rated voltage	$U_r = 220V$	Outer diameter of the cable	$\Phi = 23,4mm$
Rated power	$P_r = 150kW$	Wave's propagation speed in the cable	$w = 4020m/s$
Rated speed	$N_r = 480rpm$	Time constant of cable's internal friction	$\tau_{mp} = 0,01s$
Maximum speed	$n_{\max} = 1600rpm$	Friction coefficient of cable with water	$\beta = 0,05s^{-1}$
Armature resistance	$R_a = 0.084Ohm$	Critical tension of cable	$T = 20.000kG$
Armature current	$I_a = 745A$	Water's drag coefficient caused by vehicle's movement	$k_{no} = 1800kg/s$
Armature inductance	$L_a = 9.1mH$	Vehicle's mass in the water	$m_{no} = 5860kg$
Inertia moment	$J = 16.25Kgm^2$		
Thyristor converter			
Maximum output voltage	$U_{\mathrm{Out}} = 220V$	Time constant	$T_{In} = 0.003(s)$
Control voltage	$U_{Cont} = 10V$		

a. Synthesis of the current loop

The synthesis equations of the current control loop built based on the structure diagram shown in Figure 5 will have form:

$$W_{MC}^{k}(s) \cong \frac{W_C(s).\frac{K_{In}}{T_{In}s+1}.\frac{1/R_a}{T_a s+1}}{1 + K_C.W_C(s).\frac{K_{In}}{T_{In}s+1}.\frac{1/R_a}{T_a s+1}} \qquad (24)$$

where: $W_C(s)$ - TF of the current regulator; $W_{MC}^{k}(s)$ - the desired TF of the current loop. Solving the general equation (24) is performed with the parameters of the motor and converter given in Table 1. The TF describing the motor and converter will have the specific form:

$$W_{In}(s) = \frac{22}{3.10^{-3}s+1}; W_M(s) = \frac{11.9}{0.1s+1}.\frac{4.012}{16.25s}. \qquad (25)$$

With the desired criteria: $\sigma_{yc} = 5\%$, $t_{qd}^{yc} = 0.1(s)$, $H_\infty = 1$ the desired TF $W_{MC}^k(s)$ that is determined according to (19) will have the form:

$$W_{MC}^k(s) = \frac{0.016s + 1}{5*10^{-4}s^2 + 3*10^{-2}s + 1}, \quad (26)$$

and the feedback coefficient K_C is selected from the condition (3.7) and the principle of calculating the electric drive: $K_C = 0.005$. In the case of a PI current regulator:

$$W_C(s) = K_p^d + \frac{K_I^d}{s}, \quad (27)$$

we have to find two coefficients: K_p^d, K_I^d. Thus, it is necessary to choose two interpolation nodes (δ_1, δ_2) to ensure that equation (24) has a unique solution.

After calculating with the interpolation interval: $\delta \in [0.0001; 2], \Delta\delta = 0.1$, we will get a regulator of the form:

$$W_C(s) = \frac{0.01s + 0.11}{s} \quad (28)$$

The synthesis results of the current loop are shown in Table 2.

b. Synthesis of the speed loop.

The synthesis equation of the speed control loop containing the current loop (Figure 5) will be expressed by the relation:

$$W_{MS}^k(s) \cong \frac{W_S(s)W_{SC}^k(s).\frac{C_M}{Js}}{1 + K_S.W_S(s)W_{SC}^k(s).\frac{C_M}{Js}}, \quad (29)$$

$$W_{SC}^k(s) = \frac{W_C(s).\frac{K_{In}}{T_{In}s+1}.\frac{1/R_a}{T_a s+1}}{1 + K_C.W_C(s).\frac{K_{In}}{T_{In}s+1}.\frac{1/R_a}{T_a s+1}}$$

with, $W_{SC}^k(s)$ - the synthesized TF of the current loop. This TF with regulator (28) will have the form:

$$W_{SC}^k(s) = \frac{\frac{0.01s+0.11}{s}.\frac{22}{3.10^{-3}s+1}.\frac{11.9}{0.1s+1}}{1 + \frac{0.01s+0.11}{s}.\frac{22}{3.10^{-3}s+1}.\frac{11.9}{0.1s+1}}, \quad (30)$$

and the desired TF of the speed loop ($W_{MS}^k(s)$) determined according to the given required criteria ($\sigma_{yc} = 5\%$, $t_{qd}^{yc} = 0.2(s)$, $H_\infty = 1$) will have an explicit form:

$$W_{MS}^k(s) = \frac{0.032s + 1}{2*10^{-3}s^2 + 0.06s + 1}. \quad (31)$$

The results of solving equation (29) with $\delta \in [0.0001; 2], \Delta\delta = 0.1, K_S = 0.06$ are listed in Table 2. The speed regulator (PI) has the form:

$$W_S(s) = \frac{49.74s + 0.02}{s}. \quad (32)$$

c. Synthesis of the position control loop

The synthesis equation of the position control loop (Figure 5) is expressed as follows:

$$W_{MP}^k(s) \cong \frac{W_P(s)W_{SS}^k(s)W_{dt}(s).\frac{2\pi R_L}{is}}{1 + K_P.W_P(s)W_{SS}^k(s)W_{dt}(s).\frac{2\pi R_L}{is}}, \quad (33)$$

$$W_{SS}^k(s) \cong \frac{W_S(s)W_{SC}^k(s).\frac{C_M}{Js}}{1 + K_S.W_S(s)W_{SC}^k(s).\frac{C_M}{Js}}$$

where, $W_P(s)$ - the position regulator; $W_{SS}^k(s)$ - the synthesized TF of the speed loop. The desired TF of the position loop $W_{MP}^k(s)$ with the given required criteria: $\sigma_{yc} = 5\%; t_{qd}^{yc} = 0.5(s); H_\infty = 1$ would be of the form:

$$W_{MP}^k(s) = \frac{0.08s + 1}{0.01s^2 + 0.16s + 1}. \quad (34)$$

The results of solving equation (29) with $\delta \in [0.0001; 2], \Delta\delta = 0.1, K_S = 0.06$ are listed in Table 2. The position regulator (PD) has the form:

$$W_P(s) = 2.2s + 9.7 \quad (35)$$

3. Simulation results and Discussion

3.1. Simulation results

The main interface of the synthesis program is indicated in Figure 7, and the simulation diagram of the control system is shown in Figure 8.

1. Case 1: *The length of cable:* $L = 500m$ *, the operation depth of the UV:* $h_g = 100m$.

The calculation results are shown in Table 2, while the graphical representation of the system is shown in Figure 9.

2. Case 2: *The length of cable:* $L = 1000m$, *the operation depth of the UV:* $h_g = 500m$.

The calculation results are shown in Table 3, while the graphical representation of the system is shown in Figure 10.

3. Case 3: *The length of cable:* $L = 1500m$, *the operation depth of the UV:* $h_g = 700m$.

The calculation results are shown in Table 4, while the graphical representation of the system is shown in Figure 11.

Table 2. *The parameters of the controllers and the quality criteria of synthesized system*

Loops	Interpolation interval	Controllers	Quality criteria			
			Desired criteria		Synthesized criteria	
			$\sigma_{yc}\%$	$t_{qd}^{yc}(s)$	$\sigma_{th}\%$	$t_{qd}^{th}(s)$
Current	$[10^{-4} : 0.1 : 2]$	$W_C(s) = (0.01s + 0.11)/s$	5	0.1	1.2	0.05
Speed	$[10^{-4} : 0.1 : 2]$	$W_S(s) = (49.74s + 0.2)/s$	5	0.2	6.86	0.13
Position	$[10^{-4} : 0.1 : 2]$	$W_P(s) = 2.2s + 9.7$	5	0.5	2.97	0.48

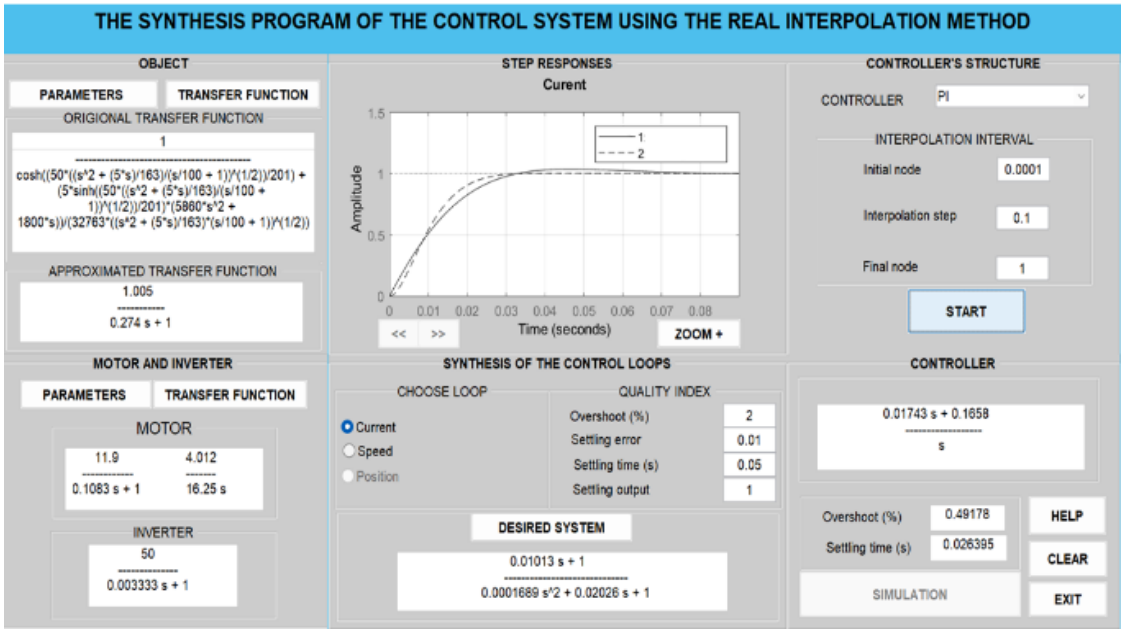

Figure 7. *The main interface of the synthesis program*

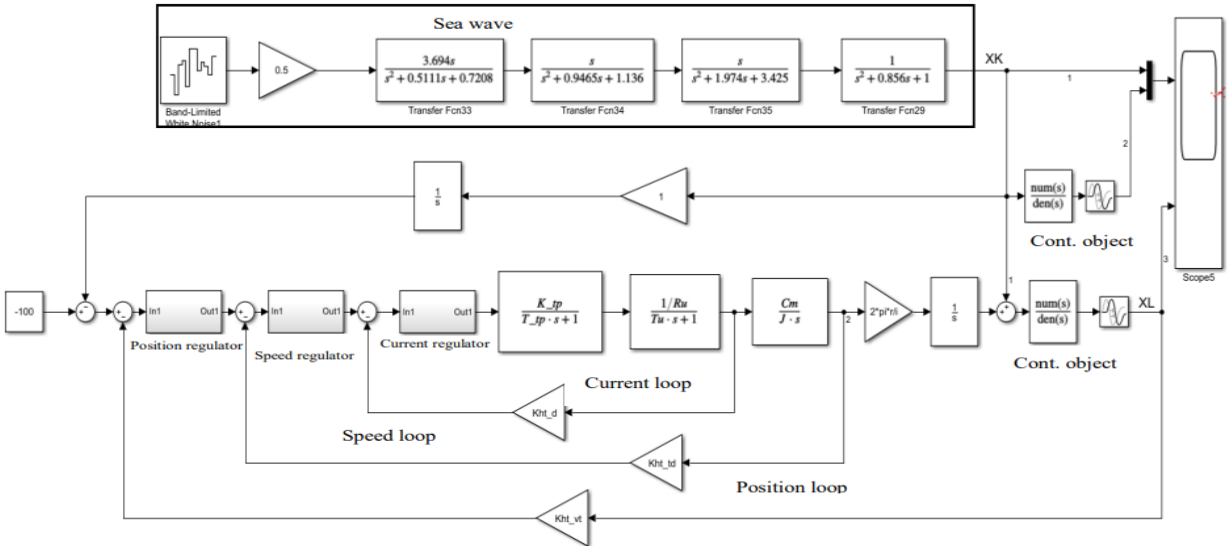

Figure 8. *The simulation diagram of the control system stabilizing the underwater vehicle under the impact of ocean waves*

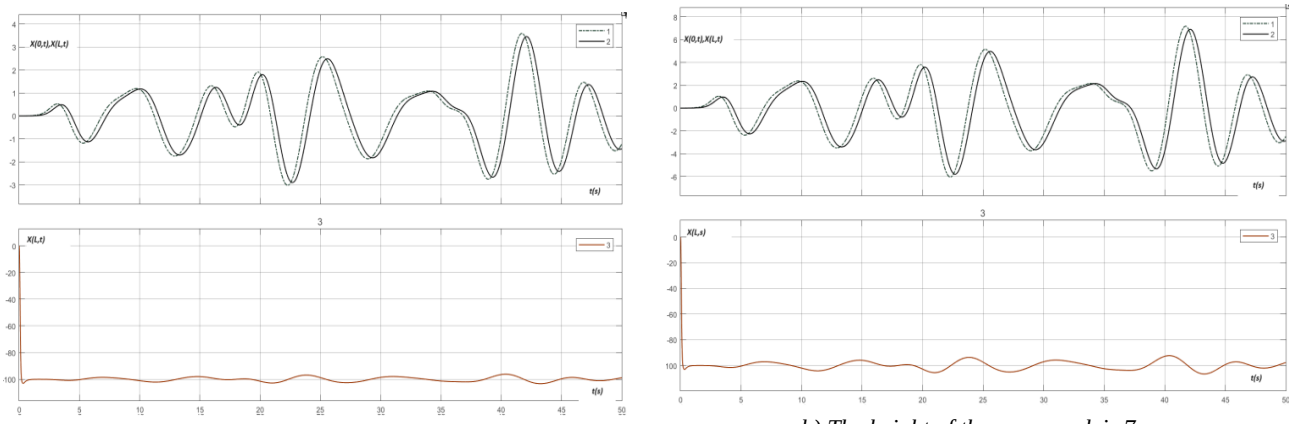

a) The height of the wave peak is 3.5m

b) The height of the wave peak is 7m

Figure 9. *The stability of UV under the impact of ocean waves at the depth 100m (The displacement at the end of cable attached to the winches $x(0,t)$ (1); The vertical displacement at the end of cable attached to the UV $x(L,t)$ without control system (2); The vertical displacement at the end of cable attached to the UV $x(L,t)$ with integrated control system (3))*

Table 3. *The parameters of the controllers and the quality criteria of synthesized system*

Loops	Interpolation interval	Controllers	Quality criteria			
			Desired criteria		Synthesized criteria	
			σ_{yc} %	$t_{qd}^{yc}(s)$	σ_{th} %	$t_{qd}^{th}(s)$
Current	$[10^{-4}:0.1:2]$	$W_C(s) = (0.01s + 0.11)/s$	5	0.1	1.2	0.05
Speed	$[10^{-4}:0.1:2]$	$W_S(s) = (49.74s + 0.2)/s$	5	0.2	6.86	0.13
Position	$[10^{-4}:0.1:2]$	$W_P(s) = 2.3s + 9.91$	5	0.5	2.45	0.42

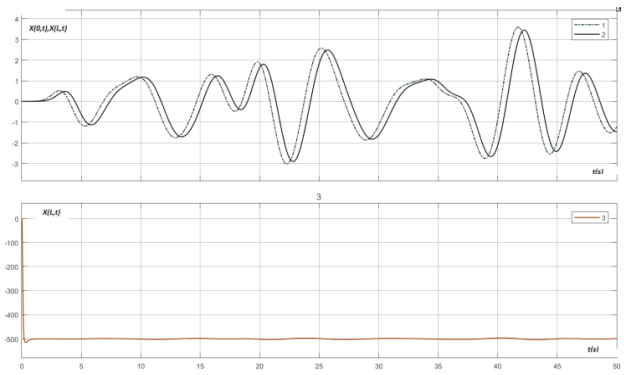

a) The height of the wave peak is 3.5m

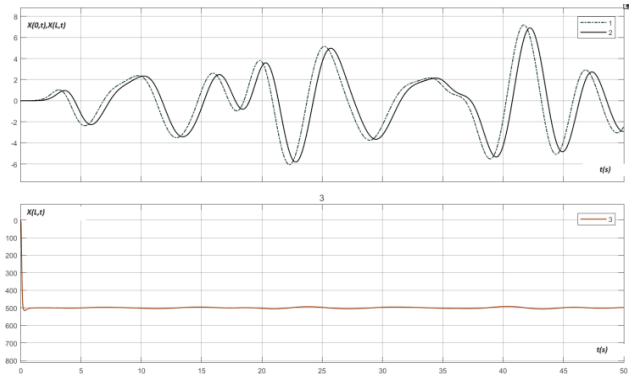

b) The height of the wave peak is 7m

Figure 10. *The stability of UV under the impact of ocean waves at the depth 500m (The displacement at the end of cable attached to the winches $x(0,t)$ (1); The vertical displacement at the end of cable attached to the UV $x(L,t)$ without control system (2); The vertical displacement at the end of cable attached to the UV $x(L,t)$ with integrated control system (3))*

Table 4. *The parameters of the controllers and the quality criteria of synthesized system*

Loops	Interpolation interval	Controller	Quality criteria			
			Desired criteria		Synthesized criteria	
			σ_{yc} %	$t_{qd}^{yc}(s)$	σ_{th} %	$t_{qd}^{th}(s)$
Current	$[10^{-4}:0.1:1]$	$W_C(s) = (0.01s + 0.11)/s$	5	0.1	1.2	0.05
Speed	$[10^{-4}:0.1:1]$	$W_S(s) = (49.74s + 0.2)/s$	5	0.2	6.86	0.13
Position	$[10^{-4}:0.1:1]$	$W_P(s) = 2.23s + 9.98$	5	0.5	3.2	0.48

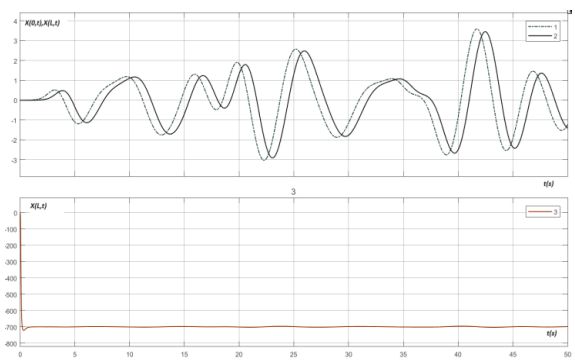

a) The height of the wave peak is 3.5m

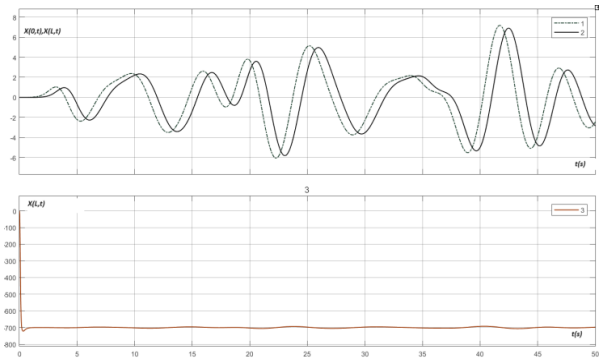

b) The height of the wave peak is 7m

Figure 11. *The stability of UV under the impact of ocean waves at the depth 700m (The displacement at the end of cable attached to the winches $x(0,t)$ (1); The vertical displacement at the end of cable attached to the UV $x(L,t)$ without control system (2); The vertical displacement at the end of cable attached to the UV $x(L,t)$ with integrated control system (3))*

3.2. Discussion

The calculation results in Tables 2,3,4 show that the received regulators meet the required quality criteria of the surveyed system, ensuring stability in both transient mode and steady mode. The analysis of graphs in Figures 9,10,11 with different cable lengths and operation depths of the UV indicates that the control system completely eliminates the influence of ocean waves with a height of less than 3m.

- For the speed control loop, the achieved overshoot is higher than the required value. This is acceptable because the working quality of the outermost control loop is most important. Therefore, although the overshoot of the speed loop (6.86%) is larger than the required overshoot (5%), it still ensures that the system works stably and satisfies the fast response.

- Simulation results show that without the control system, the oscillation amplitude of the cable end attached to the UV (line 2 in figures 9-11) will be insignificantly reduced compared to the amplitude of the cable end

attached to the winch (line 1). When integrating the control system, the oscillation amplitude of the cable end attached to the UV (line 3) is almost completely eliminated.

- The synthesized control system has the ability to completely eliminate the influence of ocean waves. With the same wave level, the stability of the UV is proportional to the cable length. This is consistent with the fact that the cable is affected by water resistance, which will eliminate the cable's oscillations.

- When the UV operates close to the ship (small cable length), the control system only works effectively at low wave levels (the wave height less than 3m). In case of rough sea (high wave height), it is necessary to move the UV away from the ship.

4. Conclusion

The solution considered in the paper provides a feasible way to solve the problem of synthesizing the control system that stabilizes the TUV under the impact of ocean waves. The proposed procedure allows direct calculations with the nonlinear functions in the real domain without converting the complex nonlinear models into the linear models. This reduces the computational amount and overall synthesis error. The calculation and simulation results show the efficiency of the proposed method without any significant difficulties. They can be used to build a control system for stabilizing the depth of TUV adjusted to ocean wave disturbances. Simulation results open up the possibility of building an adaptive control system according to changes of cable length during the operation of the UV.

REFERENCES

[1] Э.Я. Рапопорт, "*Анализ и синтез систем автоматического управления с распределенными параметрами*", М. Высш. Шк, С. 292, 2005.
(E.Y. Rapoport, "*Analysis and synthesis of automatic control systems with distributed parameters*", M. Vyssh. School, pp. 292, 2005)

[2] B. Buckham, M. Nahon, M. Seto, X. Zhao, and C. Lambert, "Dynamics and control of a towed underwater vehicle system, part I: model development", *Ocean Engineering*, Vol. 30, no. 4, pp. 453-470, 2003 https://doi.org/10.1016/S0029-8018(02)00029-X

[3] J.W. Kamman, and R.L. Huston "Multi-body dynamics modeling of variable length cable systems", *Multi-body System Dynamics*, vol 5, pp. 211-221, 2001. https://doi.org/10.1023/A:1011489801339

[4] Z. Yuan, L. Jin, W. Chi, and H. Tian "Finite difference method for solving the nonlinear dynamic equation of underwater towed system", *International Journal of Computational Methods*, Vol. 11, No. 04, 2014. https://doi.org/10.1142/S0219876213500606

[5] H. I. Park, D.H. Jung, and W. Koterayama, *"*A numerical and experimental study on dynamics of a towed low tension cable", *Applied Ocean Research*, Vol. 25, No. 05, pp. 289-299, 2003. https://doi.org/10.1016/j.apor.2004.02.003

[6] O. A. Eidsvik, and I. Schjølberg, "Time Domain Modeling of ROV Umbilical using Beam Equations", *IFAC-PapersOnLine*, Vol. 49, no. 23, pp. 452-457, 2016. https://doi.org/10.1016/j.ifacol.2016.10.447

[7] J. Gerstmayr and A.A. Shabana "Analysis of thin beams and cables using the absolute nodal co-ordinate formulation", *Nonlinear Dynamics*, Vol. 45, no. 1,2 pp. 109-130, 2006. https://link.springer.com/article/10.1007/s11071-006-s1856-1

[8] J. Gerstmayr, and H. Sugiyama, "Mikkola A. Review on the absolute nodal coordinate formulation for large defor-mation analysis of multi-body systems", *Journal of Computational and Nonlinear Dynamics*, Vol. 8, No. 03, p. 031016, 2013. https://doi.org/10.1115/1.4023487

[9] J. Park and N. Kim, *"*Dynamics modeling of a semi-submersible autonomous underwater vehicle with a towfish towed by a cable*"*, *Int. J. Nav. Archit. Ocean Eng*, Vol. 7, pp. 409-425, 2015. https://doi.org/10.1515/ijnaoe-2015-0029

[10] J.-B. Xu, B. Xin, and F. Ming, "Simulation and spectral estimation of sea wave based on shaping filter", *IEEE -The 6th International Forum on Strategic Technology (IFOST), Harbin*, 2011, pp.1243-1246. http://dx.doi.org/10.1109/ifost.2011.6021245

[11] W. Martin, and B. David van de, *"A generalized shaping filter method for higher order statistics"*, Probabilistic Engineering Mechanics, Vol. 22, no. 4, pp. 313-319, 2007. https://doi.org/10.1016/j.probengmech.2007.03.002

[12] B. M. Shameem, and V. Anantha Subramanian, "Sea wave modelling for motion control applications", *Journal of Naval Architecture and Marine Engineering*, Vol 1, No. 1, pp.29–38, 2014. https://doi.org/10.3329/jname.v11i1.17768

[13] S. Rasool, K. M. Muttaqi, and D. Sutanto, "Modelling Ocean Waves and an Investigation of Ocean Wave Spectra for the Wave-to-Wire Model of Energy Harvesting", *Engineering Proceedings*, 2021. https://doi.org/10.3390/engproc2021012051

[14] Г.Е. Кувшинов, "*Влияние морского ветрового волнения на глубоководный привязной объект*", Владивосток: Дальнаука, С. 215, 2008.
(G.E. Kuvshinov, "*The influence of sea waves on the towed underwater vehicle"*, Vladivostok: Dalnauka, pp. 215, 2008).

[15] Г.Е. Кувшинов, and К.В. Чупина, *"*Передаточная функция вертикальной качки судна*", Материалы 7 Международной научно-практической конференции"* Проблемы транспорта Дальнего Востока, 3-5 окт., 2007. - Владивосток: ДВО Рос. акад. трансп., 2007, С. 142-143.
(G.E. Kuvshinov, and K.V. Chupina, "The vertical sway transfer function of the ship", *Proceedings of the 7th International Scientific and Practical Conference "Problems of Transport of the Far East, Vladivostok,* October 3-5, 2007. Vladivostok: Far Eastern Branch of Russia. acad. transport., 2007. pp. 142-143).

[16] Г. Е. Кувшинов, "Моделирование продольной качки судна при воздействии нерегулярного морского волнения", *Проблемы транспорта Дальнего Востока*, С. 14-16, 2009.
(G. E. Kuvshinov, "Modeling the lurch of a ship under the influence of irregular sea waves", *Problems of transport of the Far East*, pp. 14-16, 2009).

[17] Г.Е. Кувшинов, and Л.А. Наумов, "Системы управления глубиной погружения буксируемых объектов: Учебное пособие для вузов", *Владивосток: Дальнаука*, С. 312, 2006.
(G.E. Kuvshinov, and L.A. Naumov, "Control systems for the depth of towed underwater objects: Textbook for universities", *Vladivostok: Dalnauka*, pp. 312, 2006).

[18] F. C. Teixeira, A. P. Aguiar, and A. Pascoal *"*Nonlinear adaptive control of an underwater towed vehicle*", Ocean Engineering*, Vol. 37, pp. 1193-1220, 2010. https://www.researchgate.net/publication/241134697_nonlinear_control_of_an_underwater_towed_vehice

[19] J. Wu, X. Yang, S. Xu, and X. Han, *"*Numerical investigation on underwater towed system dynamics using a novel hydrodynamic model", *Ocean Engineering*, Vol 247, 2022. https://doi.org/10.1016/j.oceaneng.2022.110632

[20] X. Yang, J. Wu, and S. Xu, *"Dynamic analysis of underwater towed system under undulating motion mode of towed vehicle",* Applied Ocean Research, Vol. 121, 2022. https://doi.org/10.1016/j.apor.2022.103083

[21] H. G. Kim, S. J. Yun, and J. W. Park, "Estimation and Control of a Towed Underwater Vehicle with Active Stationary and Low-Speed Maneuvering Capabilities", *Journal of Marine Science and Engineering*, Vol. 11, no. 6, pp. 1176, 2023. https://doi.org/10.3390/jmse11061176

[22] J. L. Dantas, J. J. Cruz, and E. A de Barros, "Study of autonomous underwater vehicle wave disturbance rejection in the diving plane", *Journal of Engineering for the Maritime Environment*, Vol. 228, no.2, pp.122–135, 2014. https://doi.org/10.1177/1475090213501650

[23] J. L. Dantas, J. J. Cruz, and E. A. de Barros, "Longitudinal Control of Pirajuba Autonomous Underwater Vehicle, UsingTechniques of Robust Control LQG/LTR", *IFAC Proceedings Volumes*, Vol. 43, No 20, 2010, pp. 108-113. https://doi.org/10.3182/20100915-3-DE-3008.00068

[24] В.И. Гончаров, "*Синтез электромеханических исполнительных систем промышленных роботов*", Томск: Изд-во ТПУ, С. 100, 2002.
(V.I. Goncharov, "*Synthesis of electromechanical executive systems of industrial robots"*, Tomsk: TPU Publishing House, pp. 100, 2002).

[25] V. Goncharov, I. Aleksandrov, and V. Rudnicki, "*Real Interpolation Method for Automatic Control Problems Solution*", LAP Lambert Academic Publishing, pp. 300, 2014.

[26] M. A. Abutheraa, and D. Lester, "Computable function representations using effective Chebyshev polynomial", *World academy of science, Engineering and Technology*, pp. 103-109, 2007.